Accelerated synthesis of Sn-BEA in fluoride media

effect of H2O content in the gel

Yakimov, Alexander V.; Kolyagin, Yury G.; Tolborg, Søren; Vennestrøm, Peter N. R.; Ivanova, Irina I.

Published in:
New Journal of Chemistry

Link to article, DOI:
10.1039/C6NJ00394J

Publication date:
2016

Document Version
Peer reviewed version

NJC

Accepted Manuscript

This article can be cited before page numbers have been issued, to do this please use: A. V. Yakimov, Y. G. Kolyagin, S. Tolborg, P. N. R. Vennestrøm and I. I. Ivanova, *New J. Chem.*, 2016, DOI: 10.1039/C6NJ00394J.

View Article Online
DOI: 10.1039/C6NJ00394J

Journal Name

ARTICLE

Accelerated synthesis of Sn-BEA in fluoride media: effect of H_2O content in the gel

Received 00th January 20xx,
Accepted 00th January 20xx

DOI: 10.1039/x0xx00000x

www.rsc.org/

Alexander V. Yakimov [a], Yury. G. Kolyagin[a,b], Søren Tolborg[c,d], Peter N. R. Vennestrøm[c] and Irina I. Ivanova[a,b,*]

Tin-containing zeotypes, particularly Sn-BEA, are promising heterogeneous catalysts for a number of important industrially relevant reactions. However, the direct hydrothermal synthesis of these materials requires unfavourably long times, which is an obstacle for their industrial application. In the present study we show that up to 4-fold reduction of the crystallization time can be achieved by the decreasing of the H_2O/SiO_2 ratio in the synthesis gel from 7.5 to 5.6. The crystallization kinetics has been studied for five series of gels containing 1.0 SiO_2 : 0.27 TEA_2O : x SnO_2 : 0.54 HF : y H_2O, for which y was fixed to 5.6, 6.8 and 7.7 at x = 0.005 and to 5.6 and 6.8 at x = 0.010. The crystallization time was varied within 0.5 – 60 days. The intermediate and final products obtained were investigated using XRD, FTIR, XRF, SEM, UV-Vis, MAS NMR spectroscopy and nitrogen adsorption-desorption techniques. The products obtained with lower water content are shown to have the same structure, textural properties and morphology as materials synthesized with higher water content. Although the size of the crystals is found to decrease with water content in the gel, it does not affect the Sn coordination and environment as confirmed by ^{119}Sn MAS NMR.

1. Introduction

Tin-containing zeolites and zeotypes, particularly Sn-BEA, have been demonstrated to be promising heterogeneous catalysts for many important industrially relevant reactions including the conversion of sugars into methyl lactate[1,2], the isomerization of glucose into fructose[3-5], Baeyer-Villiger oxidation reactions[6] and Meerwein-Ponndorf-Verley-Oppenauer redox reactions[7] and ring-opening hydration of epoxides[8]. In general there are a large number of examples of the widespread applicability of Sn-BEA zeolites as catalysts in biomass-derived processes[9].

The outstanding catalytic properties of Sn-BEA are considered to be due to high Lewis acidity attributed to isolated Sn atoms in the zeolite lattice and hydrophobic environment associated with defect-free siliceous surface[10,11]. The latter feature is a consequence of the fluoride route used for the synthesis of Sn-BEA materials[10]. Fluoride ions facilitate the mineralization of silica sources and compensate the positive charges associated with organic structure directing agents, which results in highly crystalline materials with a low amount of structural defects compared to materials synthesized using hydroxide ions[12]. However, the application of fluoride ions is accompanied by a number of drawbacks, including complicated handling measures of the fluoride source e.g. HF and formation of large zeolite crystals. Furthermore, the increase of Sn content in the reaction mixture, required for the creation of higher amount of Lewis sites results in long crystallization times[1]. Thus, in the case of low amounts of Sn (Si/Sn = 400) crystallization occurs within 4 days, whereas the synthesis of Sn-BEA with Si/Sn = 100 requires up to 60 days of synthesis[1].

To reduce the crystallization time and the crystal size several approaches have been proposed. These include extensive seeding[13-15], steam-assisted conversion[13] and post-synthesis modification[8,16-21]. Significant efforts have been made for shortening the crystallization time by seeded growth methods[22-24]. Although noticeable reduction of crystallization time was achieved, the induced nucleation severely affected the crystal morphology, resulting in intergrown zeolite crystals forming large agglomerates[22,24,25]. An interesting method was proposed by Chang *et al.*[23], who demonstrated that Sn-BEA can be synthesized in non-fluoride media via dry gel conversion using a seeded growth procedure. However, this approach yielded materials with a hydrophilic surface and a different distribution and location of Sn sites, as revealed by FTIR of adsorbed CD_3CN, which resulted in lower catalytic activity in glucose isomerization. Several approaches have been proposed for the preparation of Sn-BEA by post-synthesis modification[8,16-21]. All these approaches are based on the incorporation of Sn into the defects created in the BEA

[a] Department of Chemistry, Lomonosov Moscow State University, Leninskie gory 1, Moscow, Russia.
[b] A.V. Topchiev Institute of Petrochemical Synthesis RAS, Moscow, Russia.
[c] Haldor Topsøe A/S, Haldor Topsøes Allé 1, DK-2800 Kgs. Lyngby.
[d] Technical University of Denmark, Department of Chemistry, Kemitorvet, DK-2800 Kgs. Lyngby

Electronic Supplementary Information (ESI) available: [XRD, UV-Vis and adsorption data]. See DOI: 10.1039/x0xx00000x

structure during a preceding dealumination procedure. The incorporation procedures reported include grafting by chemical vapour deposition using tin chloride vapour[19,20], solid state ion exchange with tin acetate[16], dry impregnation with organometallic dimethyltin dichloride[8] and solution based methods[21]. Condensation of various tin sources with silanol defects yields the tetrahedraly coordinated tin sites. The post-synthesis procedures usually require significantly less synthesis time and produce no toxic waste in comparison to the benchmark process. Besides that, application of these procedures allows for the synthesis of materials with smaller crystal size and higher tin content[26]. However, due to the low mobility of tin sources used in the syntheses and the lack of the ability to control the type and the amount of defects generated by the dealumination process, these methods usually lead to inhomogeneous and incomplete incorporation of Sn into the framework and different Sn environment with respect to benchmark Sn-BEA materials. Furthermore, the large amount of defects formed during the dealumination procedure makes the surface hydrophilic, which is undesired in some industrial applications. Therefore the improvement of Sn-BEA synthesis and its acceleration still remains a challenge.

Retardation of zeolite synthesis in fluoride media, compared to hydroxide media, and formation of larger zeolite crystals are usually explained by a lower degree of saturation, which limits nucleation at the initial steps of the synthesis[27]. Variation of water content in the synthesis mixture has been repeatedly demonstrated as an important parameter, affecting the crystallization rate as well as crystal size and morphology of the final product[28-30]. Thus, in the case of Al-containing BEA zeolites the crystallization time was shown to decrease two-fold by decreasing the H_2O/SiO_2 ratio in the reaction mixture[29]. This approach has additionally been used for decreasing the crystal size[30] and regulation of phase selectivity of zeolite synthesis in fluoride media[31].

In this study the saturation degree in Sn-BEA reaction gel mixtures with different Si/Sn ratios is explored by varying the water content. Results show that the crystallization kinetics strongly depends on the water content and that the crystallization time can be reduced several-fold by lowering the water content. Products obtained via this accelerated synthetic route have similar Sn-sites as confirmed by ^{119}Sn MAS NMR.

2. Experimental

2.1. Synthesis of Sn-BEA

In a typical synthesis tetraethyl orthosilicate, TEOS (REAKOR, 98 wt. %) and tetraethylammonium hydroxide, TEAOH (Sigma Aldrich, 35 wt. % aqueous solution) were mixed and stirred on a magnetic stirrer until a clear solution was obtained. Then an aqueous solution of tin(IV)chloride ($SnCl_4 \cdot 5H_2O$, Sigma Aldrich, 99.9 %) was added dropwise to the template and silica solution. The mixture was stirred until the ethanol obtained during TEOS hydrolysis had completely evaporated (measured gravimetrically). Finally, hydrofluoric acid (Fluka, 40 wt. % aqueous solution) was added and the gel was homogenized by mechanical mixing. The crystallization was studied for five series of gels containing 1.0 SiO_2 : 0.27 TEA_2O : x SnO_2 : 0.54 HF : y H_2O, for which y was fixed to 5.6, 6.8 and 7.7 at x = 0.005 and to 5.6 and 6.8 at x = 0.010. After preparation the gels were transferred into Teflon-lined autoclaves that were placed in a preheated oven and kept in a preheated oven at 140°C for 0.5 – 60 days. Finally, the solid products were recovered by filtration, washed and dried at 60°C overnight and calcined in a flow of air at 550°C for 6 hours. For ^{119}Sn MAS NMR studies the samples were dehydrated at 250°C under vacuum conditions.

2.2. Characterization

The structure, morphology and texture of the intermediate and final products were studied by X-ray diffraction (XRD), Fourier-transform infrared spectra (FTIR), scanning electron microscopy (SEM), and N_2-adsorption/desorption. XRD analysis was carried out on a D2 PHASER (Bruker) diffractometer, in the range of 2θ = 5 – 50° using filtered CuKα radiation. FTIR spectra were measured on a Nicolet 600 spectrometer in the spectral region of 4000 – 400 cm^{-1}. SEM images were obtained with a scanning electron microscope LEO EVO 50XVP (Zeiss), equipped with an energy dispersive analyser INCA-energy 450 (Oxford Instruments). N_2-adsorption/desorption was carried out on outgassed samples using an ASAP-2000 (Micromeritics) instrument. The elemental analysis of the samples was performed using X-ray fluorescence (XRF) techniques over Axios MAX Advanced spectrometer (PANalytical), operating at 4 kV and using a Rh-tube. The mass fraction of Sn in the samples was determined relatively to the standard Sn(0.94%)-BEA, which was prepared by incipient wetness impregnation on the zeolite BEA using a $SnCl_4 \cdot 5H_2O$ solution. The local structure and the environment of Sn-sites were investigated by UV-Vis and MAS NMR. Diffuse reflectance UV-Vis spectra (DRUV) were recorded on Evolution 600 spectrometer using $BaSO_4$ as reference standard in the spectral region of 190 – 320 nm. For graphical representation Kubelka-Munk units was used. MAS NMR spectra were recorded on an AVANCE-II 400 (BRUKER) spectrometer with a magnetic field of 9.4 T. ^{29}Si, ^{19}F and ^{119}Sn chemical shifts were referred to $Si(CH_3)_4$, C_6F_6 and $Sn(CH_3)_4$, respectively. ^{19}F MAS NMR spectra were registered using a single-pulse sequence (90°-pulse). ^{29}Si CP/MAS NMR spectra were recorded using pulse sequence with the polarization transfer from protons to silicon (^{1}H-^{29}Si cross-polarization). For the registration of ^{119}Sn MAS NMR spectra the specific pulse sequence based on CPMG echo train acquisition (^{119}Sn CPMG/MAS NMR) described in[32] was applied.

3. Results and discussion

3.1. Effect of water content in the gel on the crystallization kinetics of SnBEA materials

The crystallization kinetics has been studied for samples prepared with Si/Sn ratios of 200 (Sn-BEA/200) and 100 (Sn-BEA/100), corresponding to a tin content of 1 and 2 wt. %,

View Article Online
DOI: 10.1039/C6NJ00704J

respectively. In the case of Sn-BEA/200 samples, the H_2O/SiO_2 ratio in the gel was kept at 5.6, 6.8 and 7.5, whereas for Sn-BEA/100 the ratio was fixed to 5.6 or 6.8 (Table 1). All the other synthesis parameters were the same as described in the experimental part. The crystallization time was varied within 0.5 – 60 days as shown in Table 1. The intermediate and final products obtained were investigated using XRD, FTIR, XRF, SEM, MAS NMR spectroscopy and nitrogen adsorption/desorption techniques.

Table 1. Products obtained from synthesis gel with molar composition: 1.0 SiO_2 : 0.27 TEA_2O : x SnO_2 : 0.54 HF : y H_2O.

Series	x	y	Crystallization time, days
1	0.005	5.6	0.5, 1.5, 4, 7, 10
2	**0.005**	6.8	0.5, 1.5, 4, 7, 10
3	**0.005**	7.5	1.5, 4, 7, 10
4	0.010	5.6	2, 4, 10, 12, 16
5	0.010	6.8	2, 4, 10, 30 ,40, 60

The results of XRD and FTIR measurements of the solid products are presented in Fig. 1 and Table 2 for the series Sn-BEA/200 (H_2O/SiO_2 = 6.8). The data obtained for the other series can be found in the Supporting information (Fig. S1 and S2).

Table 2. Characteristics of the intermediate and final products obtained in series Sn-BEA/200 (H_2O/SiO_2 =6.8).

Crystallization time, days	Si/Sn in final product[a]	Crystal-linity, %[b]	V_{total}[c]	V_{micro}[c]	Average crystal size, μm[d]	a/b
0.5	206	0	0.607	0.124	-	-
1.5	207	13	0.461	0.138	4.0	1.5
4	200	42	0.335	0.162	6.5	1.5
7	205	100	0.267	0.199	7.5	1.5
10	199	99	0.237	0.198	8.5	1.5

[a]according to XRF analysis; [b]according to XRD; [c]measured by low-temperature N_2 adsorption; [d]measured by SEM (see Fig. 5)). The crystal size is listed as an average of a minimum of 10 crystals[d].

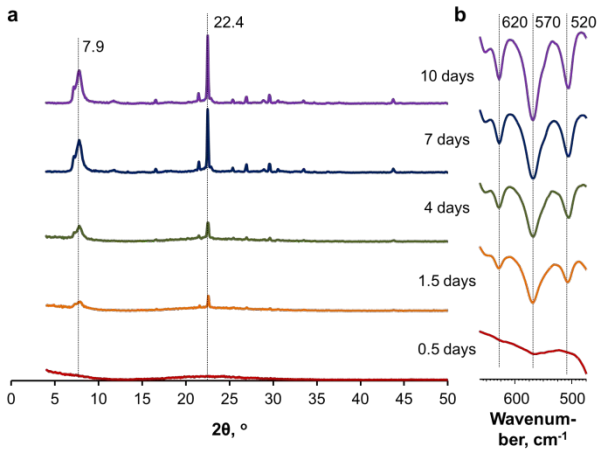

Fig. 1. XRD patterns (a) and FTIR spectra in the double-ring region (b) obtained during crystallization of Sn-BEA/200 (H_2O/SiO_2 = 6.8) samples.

At the initial phase of the synthesis (after 0.5 days) only an amorphous phase is observed (Fig. 1a). The FTIR spectrum shows a small band at ca. 570 cm^{-1}, corresponding to D4R (four-membered double-ring)[33], which points to the formation of secondary building units in the solid part of the gel, possibly due to the nucleation of zeolite.

After an increase in crystallization time the intensity of 570 cm^{-1} band increases and the appearance of other bands typical for zeolite BEA at ca. 520 and 620 cm^{-1} also become visible. The formation of zeolite BEA is confirmed by XRD, showing typical reflections of BEA structure[34] after 1.5 days of crystallization. After 7 days of synthesis a fully crystalline zeolite sample is obtained as confirmed by both XRD and FTIR data. Further increase in crystallization time does not lead to any significant changes in the XRD pattern or FTIR spectrum. The asymmetry of the peak in the range of 2θ = 7°–9° indicates a slightly uneven distribution between polymorphs A and B of the BEA structure[35]. To quantify the crystallinity the narrow diffraction peak centered at 22.35° (hkl index 330) was used, sample Sn-BEA/100 (H_2O/SiO_2 = 6.8) crystallized for 60 days was considered as 100% crystalline. The results are presented in Table 2.

Changes in the local structure of the different nuclei during crystallization were studied by MAS NMR. Fig. 2 shows the development of ^{19}F MAS NMR and ^{29}Si CP/MAS NMR spectra of the samples with increasing crystallization time. Two main signals are observed in the ^{19}F NMR spectra at ca. -59 and -70 ppm. These features correspond to fluorine atoms in two non-equivalent $[SiO_{4/2}F]^-$ configurations in as-synthesized Sn-BEA samples, where the negative charge can be balanced by the structure directing agent[35]. The intensity of the NMR lines correlates with the intensity of XRD reflections suggesting that $[SiO_{4/2}F]^-$ units are only formed in the crystalline fragments of zeolite BEA.

^{29}Si CP/MAS NMR spectra show at least five different signals corresponding to Si atoms in different local surroundings. The first group of signals in the range δ = -100 – -103 ppm corresponds to Q3-Si species mainly associated with the amorphous phase, whereas the second group of NMR lines in the range of δ = -105 – -117 can be attributed to Q4-Si in crystalline and pre-crystalline BEA phase.

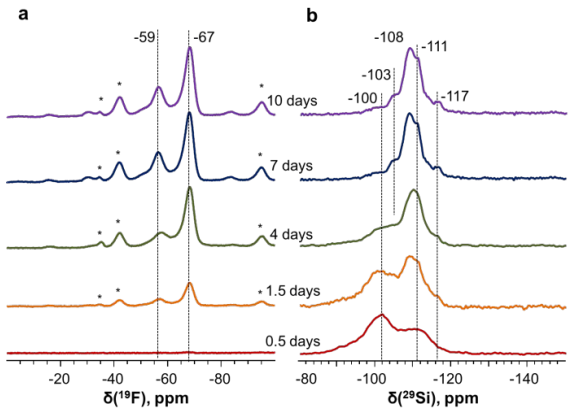

Fig. 2. Effect of crystallization time on the local structure of F and Si atoms studied by ^{19}F MAS NMR (a) and ^{29}Si CP/MAS (b) for a Sn-BEA/200 (H_2O/SiO_2 = 6.8) samples.

As the crystallinity of Sn-BEA increases, the signal features become more defined in the region of δ = -105 – -117 ppm. The increase of the intensity of the NMR lines corresponding to Q4-Si species is in line with the increase of crystallinity determined by XRD (Table 2). It is important to note that the Q4-signal in ^{29}Si CP/MAS NMR appears immediately after the beginning of crystallization. It means that $Si(OSi)_4$-species are already present in the initial gel. This is most probably due to non-alkaline media and the low amount of water in the reaction mixture compared to other zeolite syntheses.

The effect of water content in the initial gel on the crystallization kinetics is shown in Figs. 3 and 4 for the series with low and high tin content, respectively. In both cases, the decrease of H_2O/SiO_2 ratio leads to an acceleration of the crystallization process. For gels with Si/Sn=200 the decrease of H_2O/SiO_2 ratio from 7.5 to 5.6 results in a decrease of the synthesis time from 10 to 4 days (Fig. 3). In the case of gels with Si/Sn=100 a four-fold reduction of crystallization time is achieved by decreasing the H_2O/SiO_2 ratio from 6.8 to 5.6 (Fig. 4). One may suppose that further decrease of H_2O/SiO_2 ratio in the reaction mixture would lead to further lowering of synthesis times. However, further decrease of water content in the synthesis gel leads to an increase in viscosity of the gel to a point where it is difficult to homogenize by mechanical stirring. Mixing during the dissolution of tin is important in order to avoid inhomogeneities and formation of tin oxide species. As a result, it was not possible to obtain gels with lower H_2O/SiO_2 ratio than 5.6.

The comparison of the kinetic curves obtained for the samples with different Sn content in the gel at the same H_2O/SiO_2 ratio of 6.8 (Figs. 3, 4) points to the significant increase of synthesis time for the sample with higher tin content. Thus, the time required to reach complete crystallization in the case of Si/Sn = 100 is 60 days, whereas for Si/Sn = 200 only 7 days are needed, which is in good agreement with earlier data[1].

During the hydrothermal synthesis of Sn-BEA, tin atoms have been shown to form a tin-rich "shell" within the Sn-Beta crystal which was found to appear even at the early stages of crystallization[1]. During crystallization an increase in crystal size was observed together with an expansion of the enriched shell. At the same time the tin-depleted centre of the crystals also grew. These two observations point towards a dissolution-reinsertion of tin into the framework that limits the crystallization of Sn-BEA. The decrease in crystallization time with the change in water content shown in Fig. 3 and 4 imply that the dissolution-reinsertion mechanism is also affected by the saturation degree in the gel.

The analysis of the chemical composition of the intermediate and final products of crystallization (Tables 2 and 3) show equal tin contents in the solid products, which does not change with crystallization time and corresponds to nominal values. The conclusion is that all tin is present in the solid product. However, all the tin is not incorporated into the zeolite framework in samples with incomplete crystallization. Instead the tin is present as small tin oxide particles, which can be seen as bright spots in the SEM images of the intermediate products (Fig. 5). These bright spots were analysed previously using backscattered electron images[1], which confirmed the presence of tin oxide nanoparticles on the surface.

3.2. Effect of water content in the gel on the morphology and texture of SnBEA materials

The results on the changes in crystal size and morphology with crystallization time are presented in Fig. 5 and Table 2 for the series Sn-BEA/200 (H_2O/SiO_2 = 6.8). The SEM images show a gradual increase of the average crystal size from 4 to 8 μm with crystallization time, whereas the morphology of the crystals does not change. The aspect ratio between the pyramidal side (a) and the plateau (b) of the crystals remains constant ~1.5 over time, suggesting that these faces grow simultaneously. The same trend is apparent for the other series of samples. Thus, the results confirm that the nucleation occurs rather fast at the initial steps of the synthesis, which is in line with crystallization kinetics shown in Figs. 3 and 4.

The effect of water content in the gel on the crystal morphology and size is shown in Table 3 and Fig. 6. In general, an increase in the water content leads to larger crystals due to lower number of nucleation sites. For Sn-BEA with Si/Sn = 200 the crystal size increases from 3 to 12 μm with the increase of H_2O/SiO_2 ratio from 5.6 to 7.5. In the case of Si/Sn = 100 samples the effect is less pronounced, probably due to the effect of large amounts of Sn on the nucleation and crystal growth kinetics.

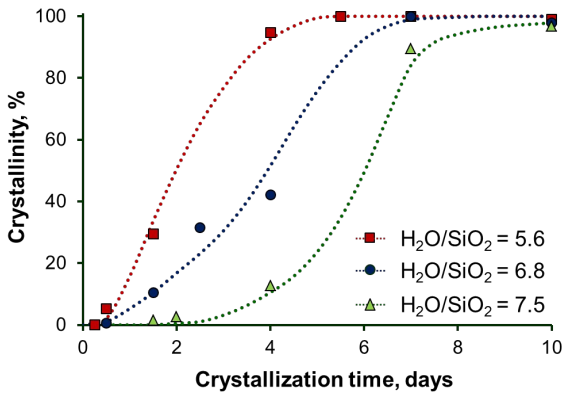

Fig. 3. Crystallization kinetics of Si/Sn = 200 gels with different water content studied by XRD.

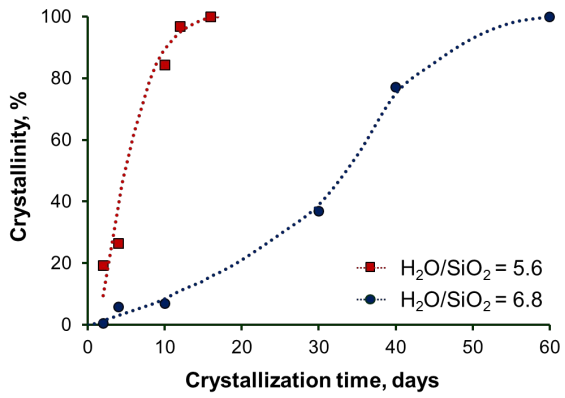

Fig. 4. Crystallization kinetics of Si/Sn = 100 gels with different water content studied by XRD.

View Article Online
DOI: 10.1039/C6NJ00394J

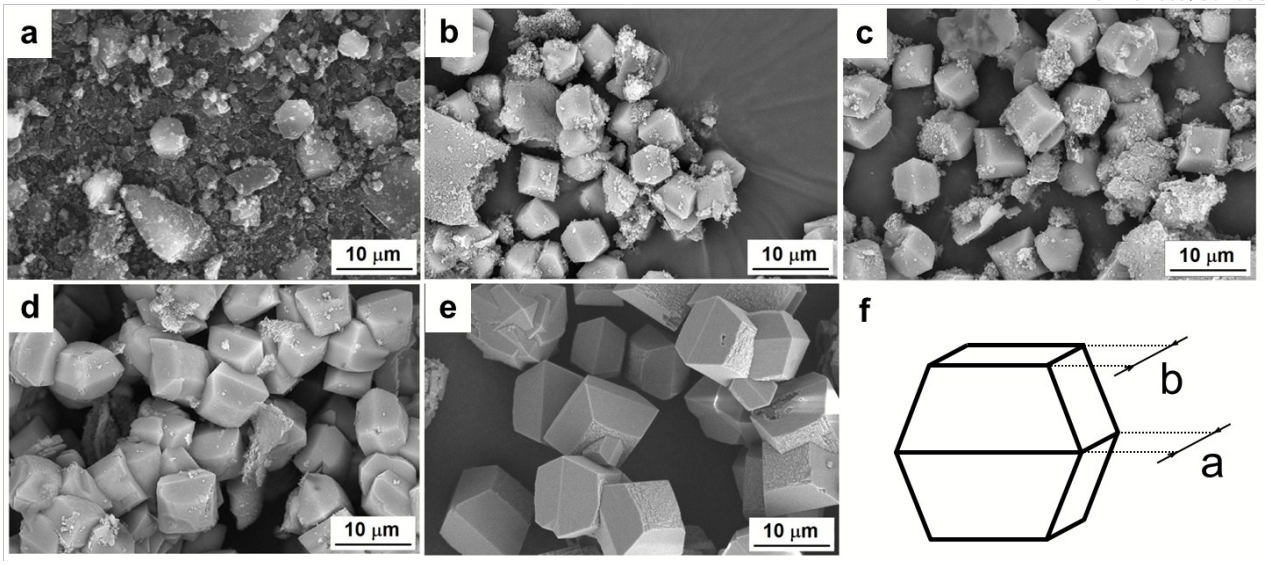

Fig. 5. SEM images of Sn-BEA/200 samples (H_2O/SiO_2 = 6.8) crystallized for 0.5 (a), 1.5 (b), 4 (c), 7 (d) and 10 (e) days. The aspect ratio of Sn-BEA crystal is schematically illustrated to explain signatures "a" and "b" (f).

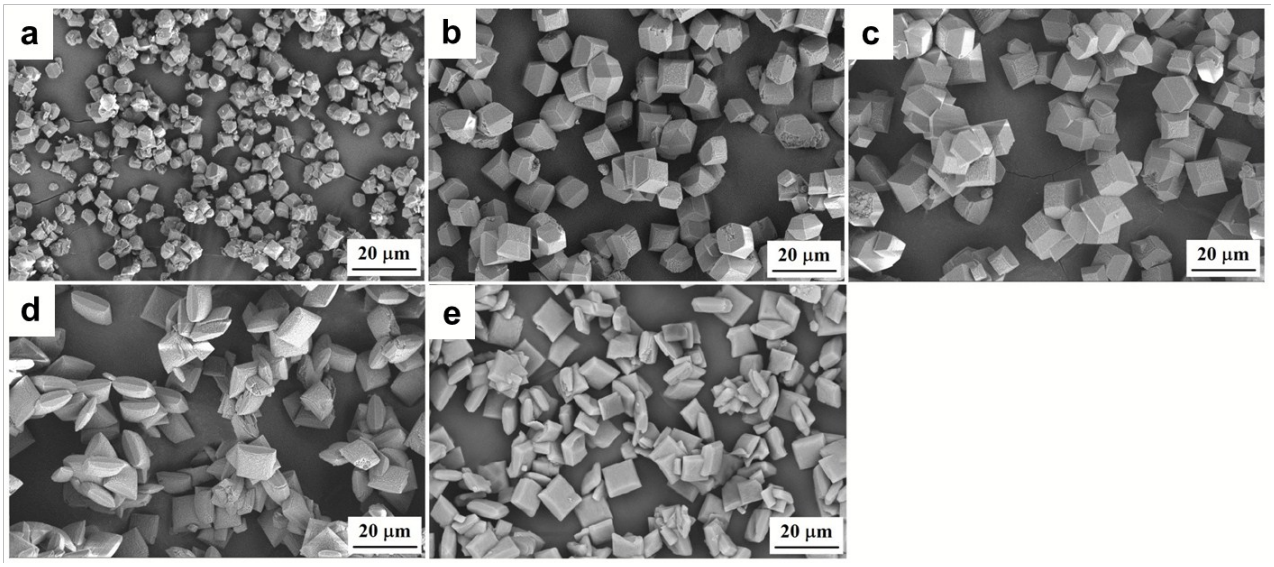

Fig. 6. Effect of water content in the gel on the morphology of the final products for Si/Sn = 200 (H_2O/SiO_2 = 5.6 (a), H_2O/SiO_2 = 6.8 (b), H_2O/SiO_2 = 7.5 (c)), and for Si/Sn = 100 (H_2O/SiO_2 = 5.6 (d) and H_2O/SiO_2 = 6.8 (e)) series.

Similar to earlier reports the aspect ratio is strongly affected by the Si/Sn ratio[1]. As the Si/Sn decreases the ratio between the pyramidal side and the plateau (a/b ratio) becomes smaller (Table 3), which again points to the effect of Sn on the growth kinetics. Additionally, it indicates that growth in the plateau direction is affected to a greater extent by the presence of Sn in the gel.

The textural properties of the intermediate and final products were studied by N_2-adsorption/desorption. The isotherms of the samples obtained during the initial steps of crystallization correspond to the amorphous products (Fig. 7a) with a large contribution of mesopores (Fig. 7b). It should be mentioned that the initial products also contain some amount of micro pores, which is an effect of fluoride ions[36]. As the crystallization time increases, the micropore volume increases and after complete crystallization the mesopores completely disappear. At this point the micropore volume also reach a plateau at the value of V = 0.2 cm^3/g (Fig. 7b) as expected for BEA zeolites.

A comparison of the textural characteristics for the fully crystalline materials in the different series show similar numbers (Table 3). All the final products show micropore volumes close to 0.2 cm^3/g, and total pore volumes in the range of 0.24 - 0.27 cm^3/g. The variation of water or tin content in the gel is therefore concluded not to affect the textural properties of the materials once a fully crystalline product is obtained.

View Article Online
DOI: 10.1039/C6NJ00394J

Table 3. Characteristics of final products obtained in the course of Sn-BEA synthesis in various conditions.

Series	Crystallization time, days	H_2O/SiO_2 in the gel	Si/Sn in the gel	Si/Sn in final producta	Relative crystallinity, %b	V_{total} c	V_{micro} c	Average crystal size, μmd	a/b
1	10	5.6	200	196	99	0.238	0.194	4.5	1.4
2	10	6.8	198	204	99	0.267	0.200	8.5	1.5
3	10	7.5	202	212	97	0.250	0.199	12.0	1.5
4	16	5.6	101	107	100	0.259	0.191	11.0	1.2
5	60	6.8	100	105	100	0.246	0.198	11.0	1.2

[a]according to XRF analysis; [b]according to XRD; [c]measured by low-temperature N_2 adsorption/desorption; [d]measured by SEM. The crystal size is listed as an average of a minimum of 10 crystals[d]

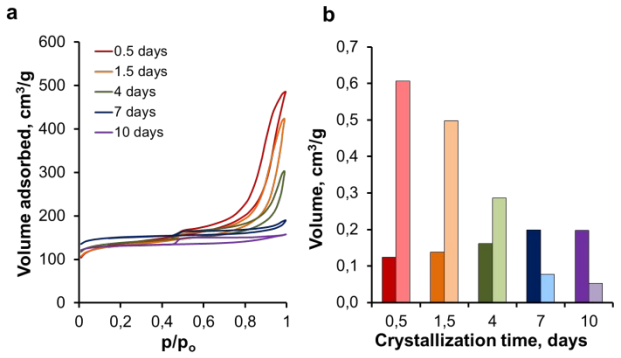

Fig. 7. Nitrogen adsorption/desorption isotherms (a) and total micropore and mesopore volume (b) in the Sn-BEA/200 (H_2O/SiO_2 = 6.8) series of samples. Deep colour corresponds to micorpore volume; pale – to mesppores.

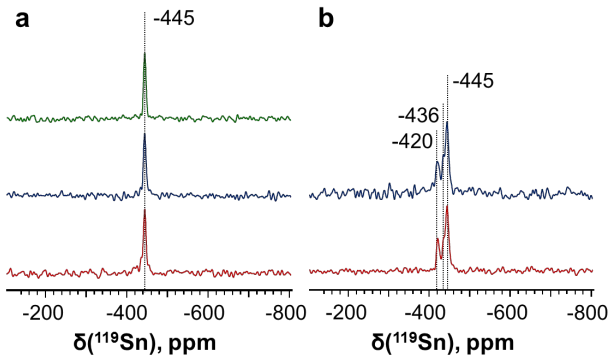

Fig. 8. ^{119}Sn CPMG/MAS NMR spectra of Sn-BEA samples crystallized from the gels with different water and tin content: Si/Sn = 200 (a), Si/Sn = 100 (b). Red lines correspond to H_2O/SiO_2 ratio of 5.6, green – 6.8 and blue – 7.5.

3.3. Characterization of Sn-sites

Since the change in H_2O/SiO_2 ratio affects the crystallization kinetics, it could be speculated that Sn is incorporated in a different manner, thus affecting the microenvironment around the Sn-site. Such an effect would alter the specific Lewis acidic properties of the final materials.

To analyze the structure of Sn sites in the final products, UV-Vis spectroscopy and ^{119}Sn CPMG/MAS NMR were applied. The UV-Vis spectra measured on fully crystalline materials are shown in Fig. S3. The results show that the Sn environment in the final products is not affected significantly by the variation of water content in the starting gel. The largest fraction of Sn is located in the framework of Sn-BEA, as confirmed by the high intensity of the band centered at ca. 205 nm. In comparison the broad band centered at ca. 280 nm, corresponding to tin dioxide is not significant.

More detailed information was obtained from ^{119}Sn MAS NMR spectra, which allowed distinguishing between different tin species in the framework (Fig. 8). In the spectra of samples with Si/Sn = 200 only one signal is observed at ca. -445 ppm, whereas in the case of the samples with Si/Sn = 100 at least 3 signals are detected at ca. -420, -436 and -445 ppm. The signals at ca. -445 ppm and -420 ppm were assigned previously to "closed" and "open" sites correspondingly[5]. The signal at ca. -436 was also reported previously[37] but was not assigned. The quantitative analysis of the spectra in Fig. 8 by the procedure reported in[32] show that the integral intensities of the signals in the case of the samples with Si/Sn = 100 are two times higher compared to Si/Sn = 200 samples, which is in line with chemical composition of the samples (Table 3). The results suggest that variation of water content in the gel does not affect the state of tin in the final products.

3.4. Discussion

The investigation of the influence of water content in the gel on the crystallization of Sn-BEA points that H_2O/SiO_2 ratio has tremendous effect on the rate of Sn-BEA synthesis and the size of crystals formed but it does not affect the structure, texture and morphology of final products as well as tin coordination and environment. According to the literature data, the mechanism of crystallization of zeolite BEA in fluoride media involves the following main stages[36:] 1) formation of primary units; 2) nucleation of zeolite BEA within the primary units; 3) aggregation and densification of the nucleated primary species; and 4) crystal growth followed by densification process. The kinetic curves presented in Figs. 3 and 4 show no induction period, which indicates that the crystallization is not limited by the formation of primary units and nucleation, but rather by the aggregation, densification and crystal growth. The comparison of the results obtained for the gels with different dilution suggest that the decrease of water content provides for higher degrees of saturation in the initial gel, which according to literature data results in faster and more complete aggregation of primary units[30], higher number of nucleation sites and lower amount of nutrient available for crystal growth[29]. As a result, the rate of crystallization is faster

in the case of concentrated gels, the amount of crystals is higher, whereas the size of crystals is smaller.

The synthetic strategy proposed leads to the following main advantages. First of all, synthesis in concentrated gels allows for significant decrease of crystallization time for Sn-BEA in fluoride media both with respect to direct synthesis in diluted gels[1] and as compared with seeded procedures[22-24]. Besides that, the decrease of water/silica ratio leads to the reduction of the size of zeolitic crystals, which is an important advantage for the catalytic application of these materials. The crystals show capped square bipyramidal morphology typical for zeolite BEA synthesized in fluoride media without intergrown parts and large crystal agglomerates, which are usually observed for the materials obtained by seeded procedures[22,24,25]. Furthermore, the synthetic strategy proposed provides for Sn-BEA materials with low amount of structural defects as compared to materials synthesized by post-synthesis modification[8,16-21]. The defect-free surface makes the material strictly hydrophobic, which results in extremely high activity and selectivity in the reactions involving moieties with different polarities[10]. Finally, the products obtained by the accelerated synthetic route show high degree of Sn incorporation and its homogeneous distribution in the framework as confirmed by ^{119}Sn MAS NMR. They contain the same type Sn-sites as benchmark Sn-BEA catalysts, which points to their high Lewis acidity and outstanding catalytic properties.

4. Conclusions

The effect of water content in the gel was demonstrated to have a significant effect on the crystallization kinetics of Sn-BEA in fluoride media. For Sn-BEA materials with Si/Sn = 200, the decrease of H_2O/SiO_2 ratio from 7.5 to 5.6 was shown to reduce the crystallization time from 10 to 4 days. In the case of SnBEA with Si/Sn = 100 the decrease of H_2O/SiO_2 ratio from 6.8 to 5.6 allowed for 4-fold reduction of synthesis time. The effect is explained by the increased degree of saturation in the initial gel with low water content, which leads to faster and more complete aggregation of primary units, higher number of nucleation sites and therefore smaller crystal size.

The analysis of the final products obtained suggests that although the size of crystals is reduced due to the decrease in water content and crystallization time, the overall aspect ratio of the capped bipyramidal primary crystals is not affected. The structure and porosity of the final products is also found to be the same. Furthermore, the analysis of Sn coordination and surroundings in the final products by UV-Vis spectroscopy and ^{119}Sn CPMG/MAS NMR showed that variation of the water content in the gel does not affect the state of Sn-sites in the final products. On the contrary, the variation of tin content in the gel has a tremendous effect on the state of tin in the framework.

Overall, the results clearly demonstrate that significant improvements to the synthesis time of Sn-BEA can be achieved by lowering the H_2O/SiO_2 ratio without compromising the state of tin in the framework.

Acknowledgements

View Article Online
DOI: 10.1039/C6NJ00394J

The authors thank the Russian Science Foundation for the financial support (grant 14-23-00094). Alexander V. Yakimov gratefully acknowledges Haldor Topsøe A/S for a PhD fellowship. Søren Tolborg is funded by the Bio-Value platform under the Danish Council for Strategic Research and The Danish Council for Technology and Innovation (Case no. 0603-00522B).

Notes and references

1 S. Tolborg, A. Katerinopoulou, D. D. Falcone, I. Sadaba, C. M. Osmundsen, R. J. Davis, E. Taarning, P. Fristrup, M. S. Holm, *J. Mater. Chem. A,* 2014, **2**, 20252–20262.
2 M. S. Holm, S. Saravanamurugan, E. Taarning, *Science*, 2010, **328**, 602–605.
3 M. Moliner, Y. Román-Leshkov, M. E. Davis, *Proc. Nat. Acad. Sci.*, 2010, **107**, 6164–6168.
4 Y. Román-Leshkov, M. Moliner, J. Labinger, M. E. Davis, *Angew. Chem. Int. Ed*, 2010, **49**, 8954–8957.
5 R. Bermejo-Deval, R. S. Assary, E. Nikolla, M. Moliner, Y. Román-Leshkov, S.-J. Hwang, A. Palsdottir, D. Silverman, R. F. Lobo, L. A. Curtiss, M. E. Davis, *Proc. Nat. Acad. Sci.*, 2012, **109**, 9727–9732.
6 M. Renz, T. Blasco, A. Corma, V. Fornes, R. Jensen, L. Nemeth, *Chem. Eur. J.*, 2002, **8**, 4708-4717.
7 A. Corma, M. E. Domine, S. Valencia, *J. Catal.*, 2003, **215**, 294–304.
8 B. Tang, W. Dai, G. Wu, N. Guan, L. Li, M. Hunger, *ACS Catal.*, 2014, **4**, 2801−2810.
9 E. Taarning, C. M. Osmundsen, X. Yang, B. Voss, S. I. Andersena, C. H. Christensen, *Energy Environ. Sci.*, 2011, **4**, 793–804.
10 R. Gounder, M. E. Davis, *AlChE J.,* 2013, **59**, 3349–3358.
11 M. Boronat, P. Concepcion, A. Corma, M. Renz. *Catal. Today*, **121**, 2007, 39–44.
12 A. Corma, M. E. Davis, *Chem. Phys. Chem.*, 2004, **5**, 304–313.
13 Z. Kang, X. Zhang, H. Liu, J. Qiu, K. Yeung, *Chem. Eng. J.*, 2013, **218**, 425–432.
14 N. K. Mal, A. V. Ramaswamy, *Chem. Commun.*, 1997, **5**, 425–426.
15 J. C. van der Waal, M. S. Rigutto, H. van Bekkum, *Chem. Commun.*, 1994, **10**, 1241–1242.
16 C. Hammond, S. Conrad, I. Hermans, *Angew. Chem. Int. Ed.*, 2012, **51**, 11736–11739.
17 P. Y. Dapsens, C. Mondelli, J. Perez-Ramirez. *Chem. Soc. Rev.*, 2015, **44**, 7025-7043.
18 J. Dijkmans, J. Demol, K. Houthoofd, S. Huang, Y. Pontikes, B. Sels., *J. Catal*., 2015, **330**, 545–557.
19 P. Li, G. Liu, H. Wu, Y. Liu, J.-g. Jiang, P. Wu, *J. Phys. Chem. C*, 2011, **115**, 3663–3670.
20 W. N. P. van der Graaff, G. Li, B. Mezari, E. A. Pidko, E. J. M. Hensen, *Chem. Cat. Chem.*, 2015, **7**, 1152–1160.
21 J. Dijkmans, D. Gabriels, M. Dusselier, F. de Clippel, P. Vanelderen, K. Houthoofd, A. Malfliet, Y. Pontikes and B. F. Sels, *Green Chem.*, 2013, **15**, 2777–2785.
22 C. Chang, Z. Wang, P. Dornath, P. Cho, W. Fan, *RSC Adv.*, 2012, **2**, 10475–10477.
23 C. Chang, H. J. Cho, Z. Wang, X. Wang, W. Fan, *Green Chem.,* 2015, **17**, 2943–2951.
24 C. M. Osmundsen, M. S. Holm, S. Dahl, E. Taarning, *Proc. R. Soc. A*, 2012, **468**, 2000–2016.
25 P. Cubillas, M. W. Anderson, in *Zeolites And Catalysis: Synthesis, Reactions And Applications*, ed. J. Cejka, A. Corma, S. Zones, Wiley-VCH Verlag GmbH & Co. KGaA, 2010, 1–55.

View Article Online
DOI: 10.1039/C6NJ00394J

26 C. Hammond, D. Padovan, A. Al-Nayili, P. P. Wells, E. K. Gibson, N. Dimitratos, *Chem. Cat. Chem.*, 2015, **7**, 3322–3331.
27 O. Larlus, V. Valtchev, *Microporous Mesoporous Mater.*, 2006, **93**, 55–61.
28 C. S. Cundy, P. A. Cox, *Microporous Mesoporous Mater.*, 2005, **82**, 1–78.
29 B. J. Schoeman, E. Babouchkina, S. Mintova, V. P. Valtchev, J. Sterte, *J. Por. Mat.*, 2001, **8**, 13-22.
30 C. Hsu, A. S. T. Chiang, R. Selvin, R. W. Thompson, *J. Phys. Chem B*, 2005, **109**, 18804-18814.
31 M. A. Camblor, L. A. Villaescusa, M. J. Diaz-Cabanas, *Top. Catal.*, 1999, **9**, 59–76.
32 Y. G. Kolyagin, A. V. Yakimov, S. Tolborg, P. N. R. Vennestrøm, I. I. Ivanova, *J. Phys. Chem. Lett.*, 2016, DOI: 10.1021/acs.jpclett.6b00249.
33 R. Hajjar, Y. Millot, P. P. Man, M. Che, S. Dzwigaj, *J. Phys. Chem. C*, 2008, **112**, 20167–20175.
34 J. B. Higgins, R. B. LaPierre, J. L. Schlenker, A. C. Rohrman, J. D. Wood, G. T. Kerr, W. J. Rohrbaugh, *Zeolites*, 1988, **8**, 446-452.
35 H. Koller, A. Wolker, L. Villaescusa, L. Diaz-Cabanas, S. Valencia, M. Camblor, *J. Am. Chem. Soc.*, 1999, **121**, 3368–3376.
36 D. P. Serrano, R. van Grieken, P. Sancez, R. Sanz, L. Rodrigez, *Microporous Mesoporous Mater.*, 2001, **46**, 35-46.
37 S.-J. Hwang, R. Gounder, Y. Bhawe, M. Orazov, R. Bermejo-Deval, M. E. Davis, *Top. Catal.*, 2015, **58**, 435–440.

View Article Online
DOI: 10.1039/C6NJ00394J

Sn-BEA synthesis in concentrated gels results in 2.5 – 4 fold reduction of crystallization time and formation of smaller zeolite crystals